Journal of Korean Society of
Coastal and Ocean Engineers
Vol. 9, No. 3, pp. 105~114, September 1997

Modeling of Circulation for the East Sea Using Reduced Gravity Models

減衰重力 模型을 이용한 東海의 循環모델링

Byung Ho Choi* and Ou Wang**
崔秉昊* · 王 歐**

Abstract Wind is one of the main forcing contributing the circulation of the East Sea. By using 1.5-layer and 2.5-layer reduced gravity models, circulation in the East Sea is simulated. The bifurcation of the Tsushima Warm Current (TWC), the separation of East Korea Warm Current (EKWC) from the east coast of Korea, the Nearshore Branch of TWC, and the cyclonic gyres stretched from the East Korea Bay to the northern half of the East Sea are compared well with the schematic map. The features of the upper and the lower layer are very similar except for those of the central region. The Polar Front is the separating line of two different features. The main feature of northern part of the East Sea, north of the Polar Front is cyclonic gyres, which are composed of three cyclonic gyres in most seasons. North Korean Cold Current (NKCC) and Liman Cold Current (LCC) are the nearshore part of these cyclonic gyres. In the south of the Polar Front the current systems of both layers are anticyclonic in most seasons, except that those of the upper layer in winter and spring are not anticyclonic. Along the coast of Korea and Russia, the velocity structure is barotropic, while that of the central region is baroclinic. The effects due to the seasonal variations of wind stress and local Ekman suction/pumping are studied by imposing the domain with modified wind stress, which is spatial mean with temporal variations and temporal mean with spatial variations. It is found that the local Ekman suction/pumping due to wind stress curl is important to the formation of the cyclonic gyres in the western and the northwestern region of the East Sea.

Keywords : circulation, the East Sea, reduced gravity model

要 旨 : 바람은 東海의 循環에 寄與하는 중요한 外力이다. 1.5層 및 2.5層 減衰重力 模型을 利用하여 東海의 循環을 시뮬레이션하여 對馬暖流의 分枝, 동해안의 東韓暖流의 分枝, 東韓灣 및 東海北部에서의 反時計方向性 循環現象을 旣存循環模型圖와 比較하였다. 上層과 下層의 樣相은 東海의 中央部를 제외하고는 類似하였는데 極前線이 다음과 같이 서로 다른 두 樣相을 제시한다. 極前線의 北側의 主樣相은 대부분의 계절에 발생하는 3개소의 反時計方向 渦動이며 이 渦動의 內側연안을 따라서 北韓寒流와 리만寒流가 흐른다. 極前線의 南側에서 上下 兩層의 海流體系는 겨울과 봄의 上層循環을 제외하고는 時計方向 循環이다. 韓國과 러시아 沿岸을 따라 流速構造는 純壓的이나 東海中部는 傾壓的이다. 바람應力의 季節的 變化와 Ekman 수송(suction/pumping)을 時間變化를 갖는 空間的平均과 空間的변화를 갖는 時間的으로 修正된 바람應力을 부여함으로서 조사하였다. 東海의 西側과 北西側 海域의 反時計方向 渦動의 形成에 있어서 바람응력 컬(curl)에 의한 局地的인 Ekman suction/pumping이 重要함을 확인하였다.

핵심용어 : 循環, 東海, 減衰重力 模型

*성균관대학교 토목공학과 (Department pf Civil Engineering, Sung Kyun Kwan University, Suwon 440-746, Korea)
**국가해양국 제2해양연구소 (Second Institute of Oceanography, SOA, Hangzhou, 311012, China)

1. INTRODUCTION

After TWC enters the East Sea, it bifurcates into two branches. The east branch is the Nearshore Branch, which flows along the coast of Japan till it exits to the North Pacific through the Tsugaru Strait. The west branch is EKWC, which flows along the east coast of Korea and then separates from the coast at about 37. 5°N. The separated EKWC flows eastward along the Polar Front in the East Sea. In the earlier modeling results, it was known that the Nearshore Branch is steered by the bottom topography and the EKWC is induced by the beta effect (Yoon, 1991). As for the problem of the separation of the EKWC from the coast of Korea, Kim and Yoon (1996) showed that the proper separation latitude is due to the existence of the northwestern cyclonic gyre by using a 1.5-layer reduced gravity model. Schematic maps show that at least one cyclonic gyre exists north of the Polar Front in the East Sea (Uda, 1934; Yarichin, 1980). The modeling results of Kim and Yoon (1996) also show a rather strong cyclonic gyre at north of the Polar Front. Although a lot of works have been done on the circulation of the East Sea, there still remain some questions to be answered. For instance; Is local Ekman suction/pumping an important role in the circulation of the East Sea? What are the different responses of the upper and the lower layer to wind forcing? By using 2. 5-layer and 1.5-layer reduced gravity models, these problems will be investigated in this study.

2. MODELS AND PARAMETERS

The models used here are 2.5-layer and 1.5-layer models that came from Hurlburt and Thompson (1980). After the primitive equations are integrated in each layer with rigid-lid and hydrostatic assumptions, the governing equations are formulated as follow,

$$\frac{\partial \vec{V}_k}{\partial t} + (\nabla \cdot \vec{V}_k + \vec{V}_k \cdot \nabla)\vec{v}_k + \vec{k} \times f\vec{V}_k \qquad (1)$$

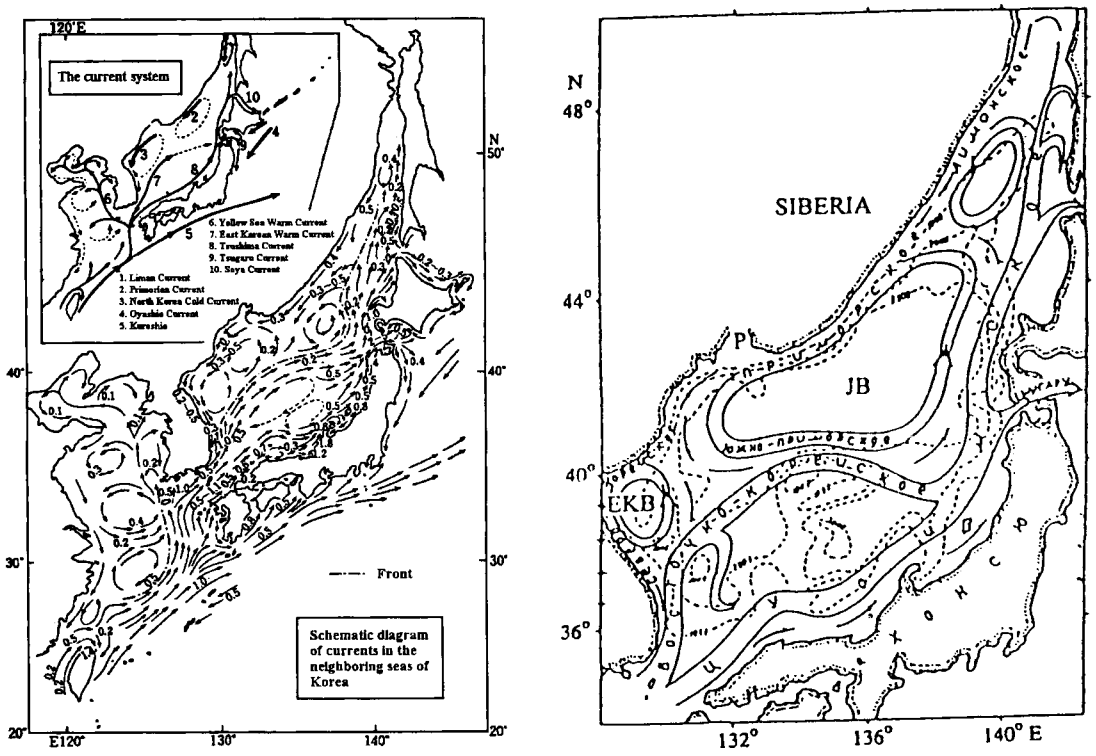

Fig. 1. Schematic maps from Uda (left) and Yarichin (right).

$$-h_k \sum_{l=1}^{2} [G_{kl} \nabla (h_l - H_l)] + (\vec{\tau}_{k-1} - \vec{\tau}_k)/\rho_0 + A_H \nabla^2 \vec{V}_k \quad (2)$$

$$\frac{\partial (h_k - H_k)}{\partial t} + \nabla \cdot \vec{V}_k = 0$$

where

k=1, 2 — k th layer,

v_k — velocity of k th layer,

h_k — thickness of k th layer at motion;,

$\vec{V}_k = h_k \vec{v}_k$ — depth-integrated velocity of k th layer,

H_k — thickness of k th layer at rest,

$G_{kl} = \begin{cases} g(\rho_3 - \rho_k)/\rho_0 & l \le k \\ g(\rho_3 - \rho_l)/\rho_0 & l > k \end{cases}$ reduced gravity,

ρ_k — density of k th layer,

$\vec{\tau}_0 = \vec{\tau}_w$ — wind stress,

$\vec{\tau}_k = \rho_0 c_k \mid \vec{v}_k - \vec{v}_{k+1} \mid (\vec{v}_k - \vec{v}k+1)$ interfacial stress of k th layer,

ρ_0 — constant reference density,

f — Coriolis parameter,

A_H — coefficient of horizontal eddy viscosity.

The finite difference scheme used is almost the same as that of Hurlburt and Thompson (1980) with a little modification. By treating the term of pressure gradient with semi-implicit scheme, we can use a larger time step. To correctly simulate the Nearshore Branch, which is induced by the bottom topography, we employ the method of Kim and Yoon (1996). The depth of the upper layer at rest decreases linearly towards the coast of Japan. Here we should point out that when treating the term of pressure gradient with semi-implicit scheme, Hurlburt and Thompson (1980) have used the depth of each layer at rest. In our situation, after we incorporate the bottom effect according to the method of Kim and Yoon (1996), the coefficient matrix to solve the equations of interfacial anomaly became an inconstant one if we used the depth of each layer at rest, which causes some computational problems. Here we prefer a constant depth when we treat the pressure gradient term with semi-implicit scheme. Results show that this modification is reasonable.

Table 1. Definition of parametes.

G_{13}=0.025 m/s^2, G_{13}=0.005 m/s^2	$\Delta x=\Delta y$=18 km, Δt=
H_1=160 m, and decrease linearly towards the Japanese coast, H_2=200 m	A_H=500 m^2/s
Q_1=2 Sv, Q_2=0 Sv, Q_1 and Q_2 are transports of upper and lower inflow in the Korea	$\rho_0=1.027\times10^3$ kg/m^3
$c_1=c_2=0$	$\beta=1.9\times10^{-11}$ m^{-1}s^{-1}

The boundary condition is non-slip condition except for the open boundary. We input a constant 2 Sv inflow at the Korea Strait. With an artificial transport distribution of 80% and 20% of the inflow of the Korea Strait to the Tsugaru Strait and Soya Strait respectively, the velocity distributions of the outflow are determined by a unique method of Hurlburt and Thompson (1980).

The parameters are shown in Table 1.

3. RESULTS AND DISCUSSION

3.1 Wind Stress and Wind Stress Curl

The wind stress data used here are from Na *et al.* (1992). Wind stress over the East Sea has strong seasonal variations (Fig. 2). During the winter, the contours of the magnitude of wind stress approximately parallel to the coastline of Russia and Korea. The center of maximum wind stress is located at off Primoriye, Russia. Wind stress off the east coast of Korea also is rather large. Compared with the relative large wind stress in winter, the wind stress in summer is less than 0.2 dyne/cm^2. The distribution of annual mean wind stress is similar to that of winter due to the weak wind stress in summer. The wind stress curl of winter has the similar features as the wind stress. The zero curl contour stretches from northeast to southwest with positive curl northwest of zero curl contour and negative curl southeast. There are two local positive maximum regions. One is located at off Primoriye and the other in the East Korea Bay. The wind stress curl of summer is very different from that of winter. The

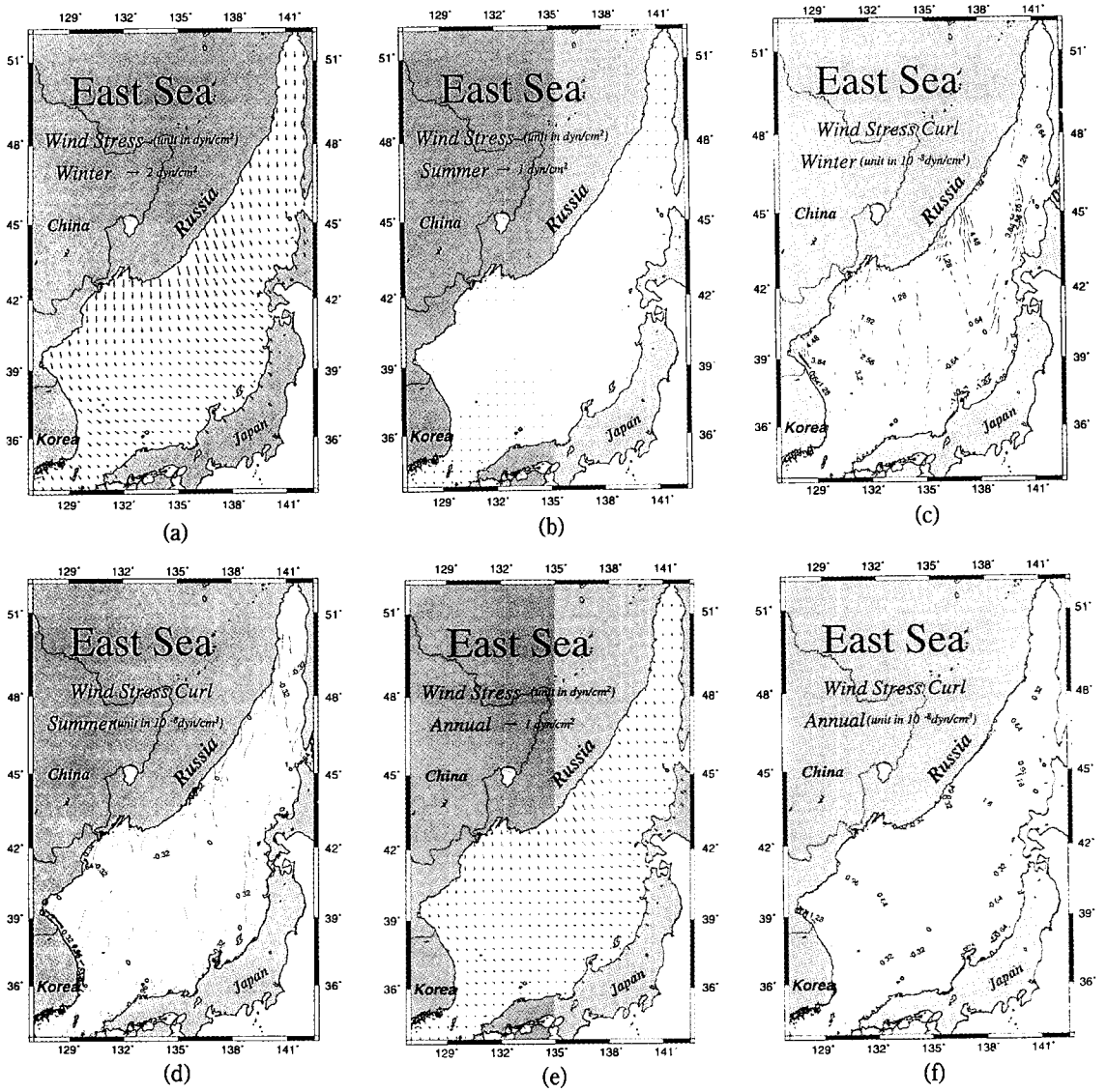

Fig. 2. Wind stress and curl in the East Sea.

local maximum centers in winter disappear and are replaced by small negative distributions in summer.

3.2 Model Results and Discussion

Presented herein are the results of four cases described in Table 2.

3.2.1 Case 1

Considering the significant difference between the distributions of wind stress in winter and summer, we can postulate that there are strong seasonal variations of the circulation in the East Sea. To show the strong seasonal variations, we give the results of February,

Table 2. Four different cases.

Case 1	2.5-layer model using wind stress from Na *et al.* (1992)
Case 2	2.5-layer model using the annual mean wind stress of Case 1
Case 3	2.5-layer model using spatial mean wind stress of Case 1
Case 4	1.5-layer model using the same wind stress as Case 1

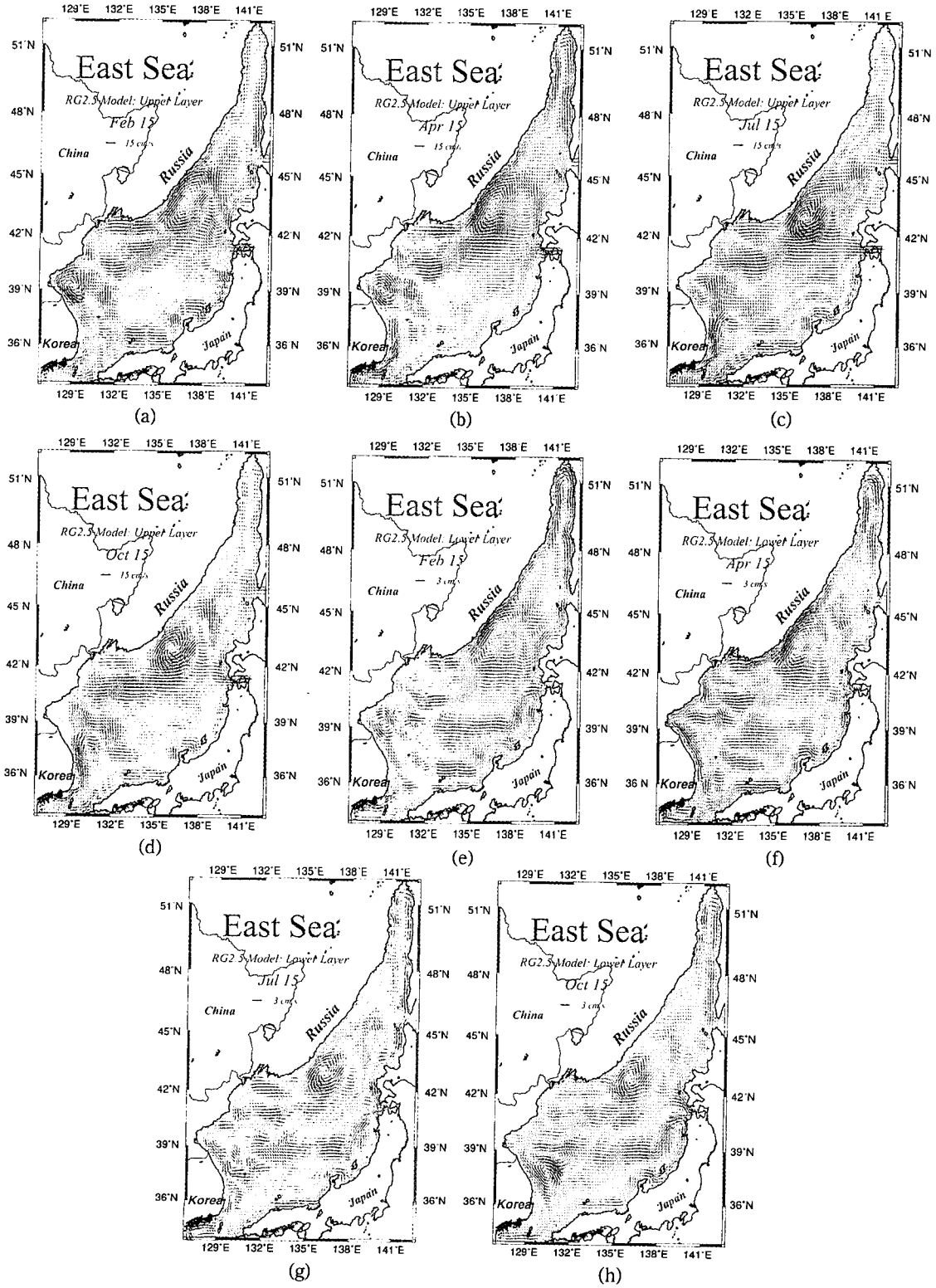

Fig. 3. Seasonal variations of the velocities in Case 1.

April, July, and October as the representative months of the circulation in winter, spring, summer, and autumn, respectively (Fig. 3).

(1) February

In the upper layer, the TWC bifurcates into two branches after it enters the Korea Strait. The EKWC flows along the east coast of Korea and separates from the coast at about 36°N, while the Nearshore Branch flows northward along the west coast of Japan. The EKWC is relatively weak. A cyclonic eddy (hereinafter referred as C1) exists north of the separation point of the EKWC. It occupies the whole East Korea Bay. The maximum velocity inside C1 reaches 15-20 cm/s. The velocity of nearshore part is larger than that of offshore part. There is a cyclonic gyre (hereinafter referred as C 2) northeast of C1. It is located at offshore of the southern part of Primoriye. Furthermore, another larger cyclonic gyre (hereinafter referred as C3) exists northeast of C2. It looks like a deformed ellipse and occupies most region of the northern half of the East Sea. NKCC and LCC are the nearshore parts of these cyclonic gyres. The most similar point of them is that the nearshore part has larger velocities than those of the offshore part, for instance, the maximum velocity of the nearshore part of C3 exceeds 20 cm/s. In the central region, the current is very weak.

In the lower layer, the circulation pattern is similar to that of the upper layer except for that of the central region. The cyclonic gyres are still clear. C3 occupies the whole northern half of the East Sea. Compared with the weak current of the upper layer in the central region, a southwestward current appears in the lower layer.

(2) April

In the upper layer, the Nearshore Branch becomes weaker at north of 37.5°N. The separating point of the EKWC is about 37°N, which shifts one degree northward from that of February. After the EKWC separates from the coast, it flows northeastward along a meandering path rather than a straight one. Another weaker northward current exists in the central region. It looks like another branch of the TWC, as suggested by some scientists.

In the lower layer, the cyclonic gyres are still clear. C3 occupies almost the whole northern half of the East Sea. In the central region, there is an anti-cyclonic feature, with a southwestward current under the northeastward current in the upper layer.

(3) July

In the upper layer, the EKWC is stronger than that in April. The separation point moves northward and reaches to 37.5°N. C1 and C2 still exist, but become weaker. In the central region, a southwestward current appears on the offshore side of the Nearshore Branch. After this southward current reaches 37°N, it turns northwestward and merges into the eastward extension of the EKWC. The Nearshore Branch is still strong after it passes through 37.5°N. Compared with that the whole northern half of the East Sea is occupied by C3 in April, now a weak anticyclonic eddy appears to the east of C3. The position of the cyclonic gyres has no significant variation except for the slightly southward shift of C2.

In the lower layer, the cyclonic gyres of C1, C2, and C3 remain. C3, which occupies the whole northern half, becomes slightly weaker. The circulation of the northernmost part has changed from the cyclonic feature to the anticyclonic one. The circulation in the whole central region is anticyclonic as that of April.

(4) October

In the upper layer, the EKWC separates from the east coast of Korea at 38°N, which shifts more northward than that of July. C1, which occupies the East Korea Bay in the other three seasons, becomes weaker and unclear. The Nearshore Branch is almost the same as that of July. The weak southwestward current in the central region has no significant changes.

In the lower layer, the cyclonic gyres become weaker, especially C1 and C2. The central region still exhibits anticyclonic features as those of April and July. The anticyclonic feature in the northernmost region is still clear.

From winter to the next autumn, the EKWC becomes stronger and the separation point from the east coast of

Korea moves northward. At least three cyclonic gyres exist both in the upper and the lower layer, although they become weaker in autumn. The Nearshore Branch in spring is the weakest one among those of the four seasons. The lower layer has some similar features to the upper layer, such as the cyclonic gyres, and certain different features as well. The most distinct feature is the circulation in the central and the northernmost regions. The circulation of the lower layer in the northernmost region is cyclonic in winter and spring while anticyclonic in summer and autumn. Along the coast of Russia and Korea, the patterns of the upper and lower layer are very similar. These similar patterns show that barotropic component of velocity is strong. In spring and winter, the directions of the currents of the upper and the lower layer in the central region are totally different. This feature shows that the baroclinic current dominates the central region in these seasons.

3.2.2 Case 2

To investigate the annual mean circulation, we impose the domain with the modified wind stress, which is annual mean with spatial variations. The main feature of the annual mean circulation (Fig. 4) is the same as the schematic map of Uda (1934). In the upper layer, the EKWC separates from the east coast of Korea at 37.5°N. To the northeast of the separation point is the cyclonic gyres. The whole northern half of the East Sea is dominated by C3. The current is very weak in the central region. In the lower layer, the position of the cyclonic gyres is the same as that of the upper layer. In the central region a cyclonic feature exhibits. This cyclonic feature is composed of a southwestward and a northward current. Recalling the weak currents in the upper layer, we deduce again that the current structure is baroclinic in the central region.

3.2.3 Case 3

The effects of local Ekman suction/pumping on the formation of the cyclonic gyres, one of the main features in the East Sea, are investigated by imposing the domain with modified wind stress. We obtain this modified wind stress by spatially averaging wind stress inside the polygon, which is composed of the coast of

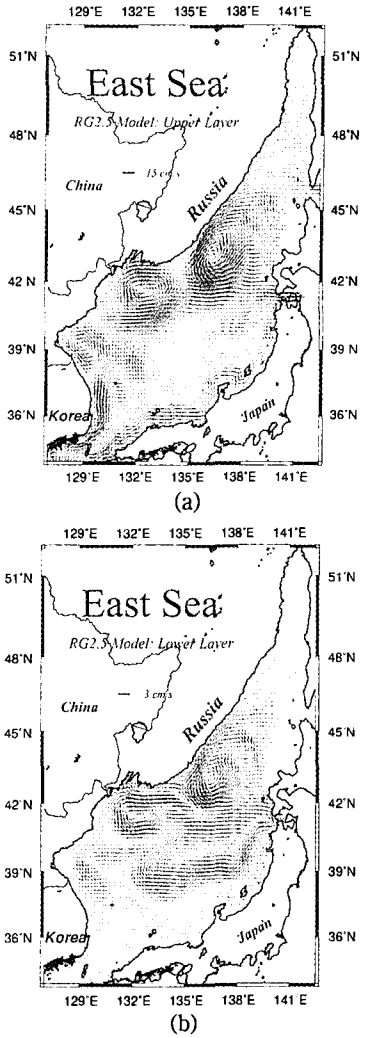

Fig. 4. Wind stress and curl in the East Sea.

Russia and Korea and the thick line, and still keep the temporal variation of the wind stress in this subregion (Fig. 5). By employing this method, we separate the effects of local Ekman suction/pumping from those of pressure head that is created by the pileup of waters from wind stress. In the upper layer, the EKWC has the same separation feature as that of Case 1, which from winter to autumn the separation point moving from south to north. The cyclonic gyres become weaker in summer and next autumn, which means the local Ekman suction/pumping is important to the formation of the cyclonic gyres, especially in summer

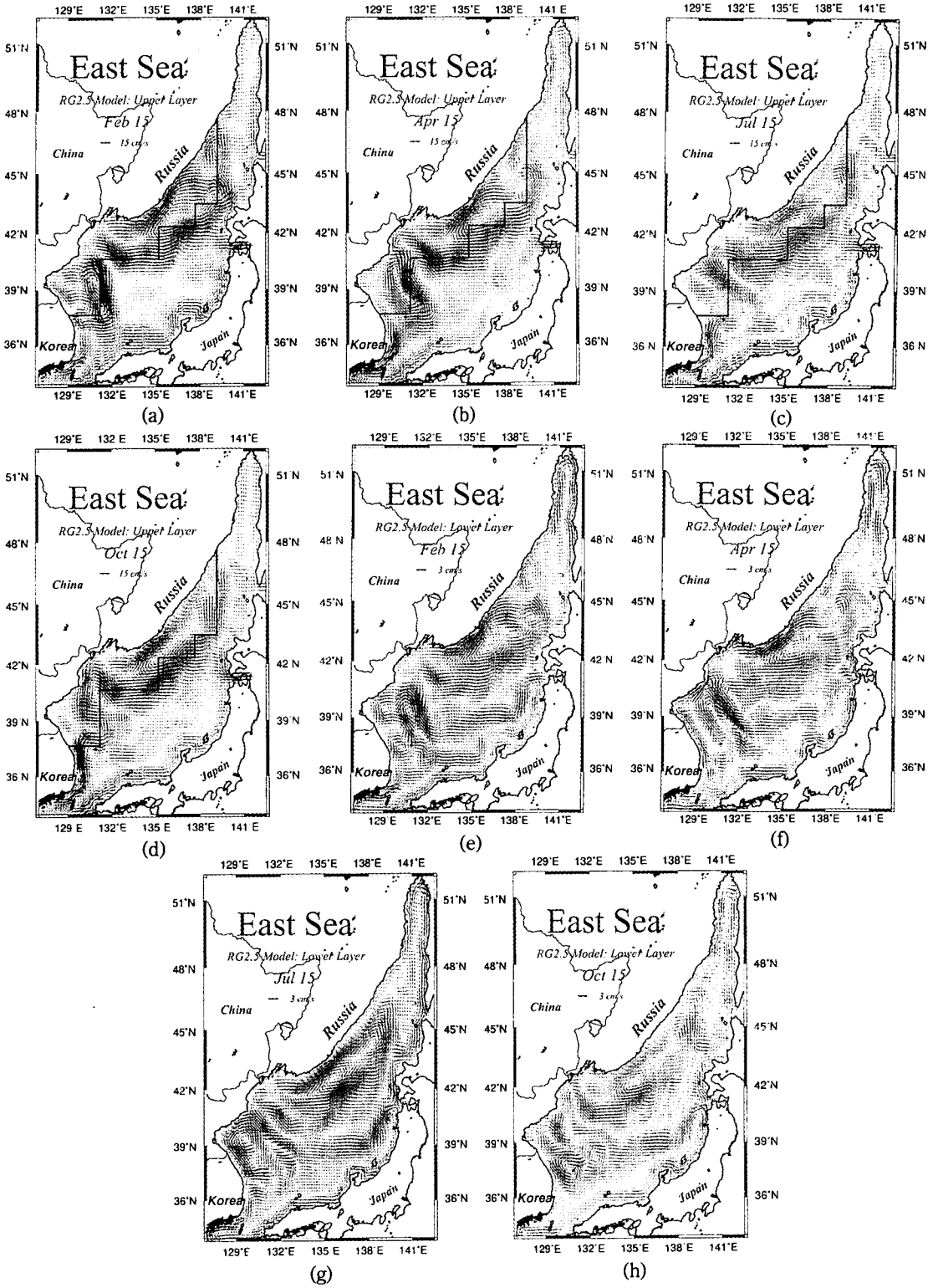

Fig. 5. Seasonal variations of the velocities in Case 3.

and autumn. The Nearshore Branch has few changes compared with that of Case 1, which means the external effects of Ekman suction/pumping on the formation of the Nearshore Branch are relatively weak. Also, the seasonal variations of the cyclonic gyres in the lower layer become weaker but still exhibit the same features as those of Case 1.

3.2.4 Case 4

We experimented the 4th case with the same wind stress as Case 1 to compare the results of 1.5 and 2.5-layer reduced gravity models. The reduced gravity G_{12} used in the 1.5-layer reduced gravity model equals 0.020 m/s^2. The features, such as the separation of the EKWC, the cyclonic gyres, and the Nearshore Branch are similar to those of the upper layer of Case 1 (Fig. 6). C1 becomes stronger than that of the upper layer of Case 1.

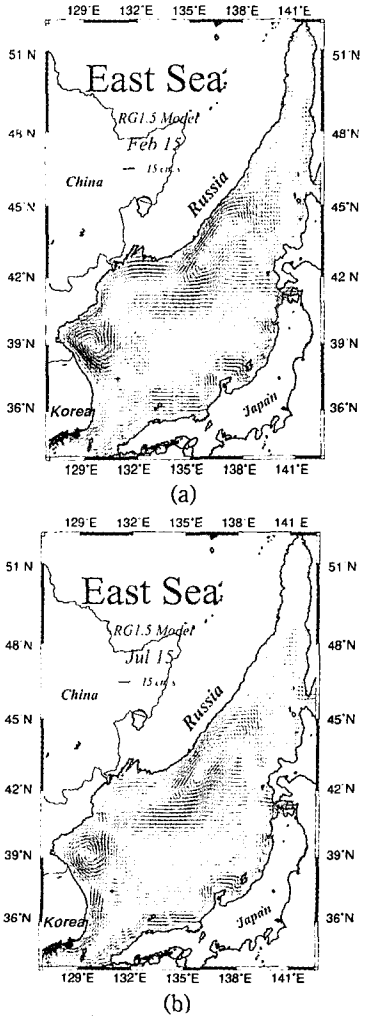

(a)

(b)

Fig. 6. Seasonal variations of the velocities in Case 4.

4. CONCLUSIONS

Circulation in the northern half of the East Sea is significantly influenced by winds. We investigated the different effects of winds using reduced gravity models. When imposed with realistic wind stress, the separation point of the EKWC shows strong seasonal variations. From winter to next autumn, the separation point moves from 36°N to 38°N. In the mean time, the EKWC becomes stronger. The Nearshore Branch in spring is the weakest one of the four seasons. There are cyclonic gyres north to the separation point both in the upper and lower layer. In summer and autumn, the circulation in the central and the northernmost regions of the East Sea is anticyclonic both in the upper and the lower layer. In the remainder seasons, the anti-cyclonic features become weaker in the upper layer, but anticyclonic circulation still dominates the central and northernmost region in the lower layer. Along the coast of Russia and Korea, the velocity structure is barotropic, however, that of the central region in winter and spring is baroclinic. When we impose the domain with annual mean wind stress, the results still correspond well with the schematic maps of Uda (1932) and Yarichin (1980). The effects of local Ekman suction/pumping are important for the formation of the cyclonic gyres. The remote forcing of Ekman suction/pumping is unimportant to the Nearshore Branch. The 1.5-layer reduced gravity model shows stronger cyclonic gyres than those of the upper layer in the 2.5-layer reduced gravity model.

REFERENCES

Hurlburt, H.E. and Thompson, J.D., 1980. A numerical study of Loop Current intrusions and eddy shedding, *J. Phys. Oceanogr.*, **10**, pp. 1611-1651.

Kim, C.-H. and Yoo, J.-H., 1996. Modeling of the wind-driven circulation in the Japan Sea using a reduced

gravity model, *J. Oceanogr.*, **52**, pp. 359-373.

Metzger, E.J. and Hurlburt, H.E., 1996. Coupled dynamics of the South China Sea, the Sulu Sea, and the Pacific Ocean, *J. Geophys. Res.*, **101**, pp. 12331-12352.

Naganuma, K., 1977. The oceanographic fluctuations in the Japan Sea, *Mar. Sci.* (Kaiyo Kagaku), **9**, pp. 137-141 (in Japanese with English abstract).

Na, J.-Y., Seo, J.-W. and Han, S.-K., 1992. Monthly-mean sea surface winds over the adjacent seas of the Korean Peninsula, *J. Oceanol. Soc. Korea*, **27**, pp. 1-10.

Uda, M., 1934. The results of simultaneous oceanographical investigations in the Japan Sea and its adjacent waters in May and June, 1932, *J. Imp. Fish. Exp. Sta.*, **5**, pp. 57-190 (in Japanese with English abstract).

Yarichin, V.G., 1980. Study state of the Japan Sea circulation, In: *Problems of Oceanography* edited by V. Pokudov, Hydrometeoizdat, Leningrad, pp. 46-61 (in Russian).

Yoon, J.-H., 1982a. Numerical experiment on the circulation in the Japan Sea, Part I. Formation of the East Korean Warm Current, *J. Oceanogr. Soc. Japan*, **38**, pp. 43-51.

Yoon, J.-H., 1982b. Numerical experiment on the circulation in the Japan Sea, Part III. Mechanism of the nearshore branch of the Tsushima Current, *J. Oceanogr. Soc. Japan*, **38**, pp. 125-130.